Synthesis and characterisation of graphene-reinforced AA 2014 MMC using squeeze casting method for lightweight aerospace structural applications

Pazhani, A., Venkatraman, M., Xavior, M. A., Moganraj, A., Batako, A., Paulsamy, J., Jayaseelan, J., A, A. & Bavan, J. S

Synthesis and characterisation of graphene-reinforced AA 2014 MMC using squeeze casting method for lightweight aerospace structural applications

Ashwath Pazhani [a], M. Venkatraman [b], M. Anthony Xavior [b],*, Arivarasu Moganraj [c], Andre Batako [d], Jeyapandiarajan Paulsamy [b], Joel Jayaseelan [b], Arivazhagan Anbalagan [e], Jayesh Shanthi Bavan [a]

[a] Faculty of Engineering, Environment and Computing, Coventry University, CV1 5FB, United Kingdom
[b] School of Mechanical Engineering, Vellore Institute of Technology, Vellore, Tamil Nadu 632014, India
[c] Centre for Innovative Manufacturing Research, Vellore Institute of Technology, Vellore, Tamil Nadu 632014, India
[d] General Engineering Research Institute, LJMU, Liverpool L3 5UX, United Kingdom
[e] Institute for Advanced Manufacturing & Engineering (AME), Coventry University, Coventry CV6 5LZ, United Kingdom

HIGHLIGHTS

- Homogeneous dispersion of nano 2D – Gr_{np} in an aluminium matrix is achieved by reinforcing a synthesized novel mixture with embedded and interlocked 2D – Gr_{np}.
- This research focuses on development of isotopic composite material aimed for launch vehicle Super Lightweight fuel Tank (SLWT) Structural Application.
- 0.5 wt% 2D – Gr_{np} and its homogeneous dispersion facilitated homogeneous nucleation of the stable θ-Al_2Cu intermetallic precipitate which resulted in improved mechanical properties compared to the pure alloy.
- A successful isotropic composite material is created and three major strengthening mechanisms are responsible for the enhancement in the mechanical properties were (1) precipitation hardening, (2) grain refinement strengthening and (3) dispersion strengthening.
- This innovation of synthesizing novel mixture with embedded and interlocked 2D – Gr_{np} and reinforcing them to achieve homogenous dispersion creates a pathway in fabricating large scale isotropic composite materials that can be used in aerospace and space exploration

GRAPHICAL ABSTRACT
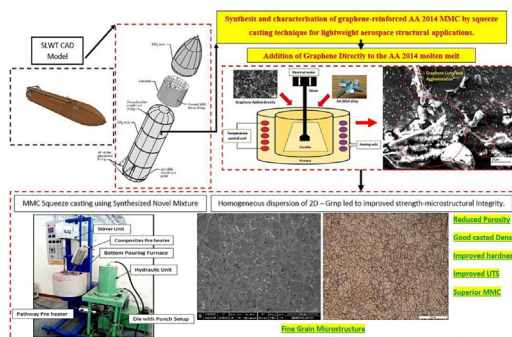
* Corresponding author.
  E-mail address: manthonyxavior@vit.ac.in (M. Anthony Xavior).

applications as an alternate material for light weighting with improved properties.

ABSTRACT

The need for lightweight materials towards aerospace has increased prominently. This paper focuses on introducing a novel reinforcement mixture of graphene with Al 2014 powder synthesised through ball milling technique. The synthesized powder was utilized as a reinforcement to fabricate Al 2014 based MMCs through squeeze casting technique. The results exhibited that Al 2014 mixture with embedded and interlocked 2D-Gr_{np} (2.517 g/cm^3) matched the density of the matrix metal (2.771 g/cm^3) that facilitated homogeneous dispersion of 2D-Gr_{np} and solved the dispersion problems during stir casting. As a result, AA 2014 embedded with 2D-Gr_{np} acted as a carrier to homogeneously disperse combined with the squeeze casting process leading to the production of homogeneously reinforced MMC. This can be considered as a potential fabrication route for the launch vehicle super lightweight fuel tank (SLWT) structural application. The final casted plate after T6 heat treatment with 0.5 wt% 2D-Gr_{np} exhibited an improved tensile strength of 361 MPa (52% higher than the monolithic 2014 aluminium alloy) with total elongation of 21% and improved hardness of 119 HRB (45.5 % increase). Furthermore, SEM and TEM results exhibited that squeeze casting led to enhanced interfacial bonding between the 2D-Gr_{np} and Al 2014.

1. Introduction

Aluminium alloy (AA) 2xxx series and their metal matrix MMCs (MMCs) have great potential as an alternate super lightweight material in aerospace and space exploration application and has gained tremendous attention among researchers due to their improved strength, heat treatability, formability, reduced density, improved fracture toughness at cryogenic temperatures and abundant availability of resources of matrix material at fair cost per kilogram (cost/kg) [1–3]. Particularly, various researchers reported that AA 2014 with reinforcements could be considered for various structural applications owing to its improved strength-microstructural integrity [4–6]. Further, AA 2014 is a heat-treatable alloy which exhibits increased strength properties and has unique microstructural characteristics when heat treated [5]. With these advantages, it is quite necessary to engineer the microstructure of the developed metal matrix that can further enhance the strength-microstructural integrity for various applications [5]. Engineering such novel nanocomposites with fine grain microstructure, enhanced particulate-matrix interfacial bonding and improved overall density for aerospace and space exploration structural application needs a careful selection of reinforcement type that needs to be reinforced with matrix metal AA 2014 [6–7].

Among various other carbides and oxides forms of ceramic reinforcements, graphene is considered as one of the promising materials to reinforce MMCs which are utilized for aerospace and space exploration applications [3,6]. 2D – Graphene nano particulates exhibit hybrid sp^2 orbital characteristics with strongly bonded carbon atoms that are found in a single layer with a hexagonal positioned structure. Gr_{np} is one of the strongest materials in the market, which exhibits an ultimate tensile strength of 130 GPa, Young's modulus of 1 TPa [4–5], superior thermal conductivity of 5000 W m^{-1} K^{-1}, higher specific surface area of 2630 m^2 g^{-1}, superior electrical conductivity of upto 100 MS/m [5–6] and with low density of 2.2 g cm^{-3} [7] Gr_{np} is considered as an effective reinforcement material for Al-based MMC. Reinforcing Gr_{np} with higher specific surface area provides improved particle to particle interfaces with enhanced load transfer mechanism, making it superior to single walled or multi walled carbon nanotubes for fabricating MMCs [8]. To meet the fuel tank structural application demand and their property requirements and to utilize the excellent mechanical properties with full potential offered by reinforced graphene not more than 0.5 wt% [9–11], is required to disperse the reinforced Gr_{np} homogeneously and achieve strong interfacial bonding in the final MMC plate.

Considering the MMC processing and fabrication routes, recent research studies have highlighted and emphasized on using solid-state powder processing routes like hot pressing [9–12], microwave sintering and spark plasma sintering [13], surface processing routes like friction stir processing and pressure infiltration routes [14–15] are majorly used to produce 2D – Gr_{np} reinforced aluminium MMCs. However, these solid-state processing routes have the capability to support the fabrication of MMCs only in small-sized components and are highly expensive. Thus, for fabricating MMCs at a larger scale towards structural applications, a liquid metallurgy route like stir casting or squeeze casting methods are the only viable options [9,16]. Compared to solid-state MMC manufacturing methods, liquid in-situ manufacturing methods exhibits various process advantages like improved yield, low manufacturing cost and simple operational flow that make it more reliable to fabricate MMCs [17 –18]. Although with these advantages, researchers and manufacturing companies feel unfortunate to fabricate nanoparticles reinforced MMCs owing to its significant density mismatch, which leads to poor wettability during the stirring process and the 2D – Gr_{np} tend to float on the molten alloy pool making the liquid fabrication route a great challenge to make as a commercial regular production route [6,10,19].

To fabricate a MMC with homogeneously dispersed Gr_{np}, various researchers have employed powder processing methods using high energy planetary ball milling (HEPBM) techniques which may facilitate dispersion of low dense 2D – Gr_{np} homogeneously in the aluminium matrix metal by superior shear forces [9,20]. During the HEPBM process lower speed ball milling facilitates uniform dispersion of 2D – Gr_{np} onto the surface of aluminium powder by providing sufficient shear force and causing the 2D – Gr_{np} to embed and cold weld onto the deformed aluminium powder at higher speed ball milling [13]. In addition, 2D – Gr_{np} dispersion efficiency majorly influenced by total ball milling duration. Various researchers have reported that the longer ball milling duration facilitates uniform dispersion as well as reducing the stacked 2D – Gr_{np} layers [8,11]. Furthermore, stacked 2D – Gr_{np} in ideal conditions with poor surface tension also influences the wettability and interfacial bonding of them to the matrix metal that creates a fabrication difficulty using any casting technique [9,21–23]. Due to this phe-

nomenon, it is quite challenging to introduce 2D – Gr$_{np}$ into the molten matrix metal whirlpool during stirring directly [12,24–26].

To overcome the issue of achieving homogeneous dispersion of graphene nanoparticles onto the Al matrix, various researchers have tried to embed powder processing into the liquid in-situ routes to fabricate MMCs. In our previous research, MMC mixtures were processed using 2D – Gr$_{np}$-aluminium powder through powder metallurgy and have improved the overall properties of the MMC compared with the monolithic alloy [27,28]. The processed powder mixture with reinforced nano 2D – Gr$_{np}$ were processed with high energy ball milling and ultra-sonication which exhibited homogenous dispersion of 2D – Gr$_{np}$ in the matrix aluminium alloys like 2024, 2219, 2014 and 6061 as well as good interfacial bonding among the dispersed 2D – Gr$_{np}$ and by forming active stable precipitates (Al$_2$Cu and Al$_2$CuMg) at the grain-reinforcement-matrix interface, respectively [27,28].

In this research work, integration of powder processing and liquid metallurgy is carried out. The in-situ processed novel powder mixture of aluminium parent alloy 2014 powder with 0.5 wt% 2D – Gr$_{np}$ is synthesised through HEPBM followed by adding the mixture to the stir casting stir molten pool to fabricate the MMCs through stir followed by squeeze casting technique. The mixture with parent alloy 2014 with 0.5 wt% of 2D – Gr$_{np}$ facilitated and solved the issue of density mismatch between the 2D – Gr$_{np}$ and 2014 matrix alloy and the floating issue of 2D – Gr$_{np}$ when added to the stir pool during the process. By using the mixture during the stir-cum-squeeze casting process the MMC with homogenously dispersed 2D – Gr$_{np}$ was produced in solid casted billets and can be hot rolled into bigger MMC plates and in large scale which will create a new pathway to fabrication technology to fabricate aluminium based MMC that can be more suitable as a potential replacement for the SLWT structural applications which may reduce the overall weight of the launch vehicle in a significant amount making space travel more cost and fuel-efficient while meetings the strength and ductility requirements. In this paper, along with the fabrication of MMC various other microstructural investigations and mechanical properties were performed to evaluate the influence of the novel mixture.

2. Experimental procedures

2.1. In-situ synthesis of the 2D – Gr$_{np}$/AA 2014 novel powder mixture

Fig. 1 illustrates the process schematic of novel mixture synthesis and the 2D – Gr$_{np}$/AA 2014 MMC using the squeeze casting process. 2D – Gr$_{np}$ nano-particulate in the form of a flaky structure with dimensions of ∼10 μm in length and width and 5 nm in thickness was procured from Angstron Materials Inc USA. and used as a main constituent in preparing the novel mixture. AA 2014 powder

with particle size ∼25 μm and density of 2.80 g/cm^3 was used as supporting material to produce the reinforcing particulates due to its closer density match with the matrix (2.76 g/cm^3) which is considered towards the fabrication of MMCs. The 2D – Gr$_{np}$ with overall density of 2.267 g/cm^3 of 0.5 wt% (5 g) and AA 2014 powder (20 g) with a mixture ratio of 1:4 has been processed through a HEPBM technique using tungsten carbide balls in them with a ball to powder ratio of 5:1. The HEPBM process was conducted in two modes, one with low speed of 150 rpm for 2 h followed by high speed of 320 rpm for 1 h. AA 2014/2D – Gr$_{np}$ mixture mechanically mixed by HEPBM process was carefully transferred to an airtight container to prevent oxidation.

The synthesized powder mixture was used in the stir casting process along with AA 2014 to fabricate the 2D – Gr$_{np}$ reinforced MMCs. The overall mixture density was calculated to be 2.56 g/cm^3 through Archimedes method by using a solid compact made out of the synthesized mixture by following ASTM standard ASTMB311-22 [23]. Fig. 2(a and b) show the field emission scanning electron microscopy (FESEM) of the as procured 2D – Gr$_{np}$ flakes and the AA 2014 powder. Table 1 provides the chemical composition of the AA 2014 powder and as received Ingot in as procured condition by using a handheld portable X-ray fluorescence (XRF) analyzer.

2.2. Squeeze casting of the 2D – Gr$_{np}$/AA 2014 MMC

Aerospace grade aluminium alloy 2014 was selected as the primary matrix material for this research study. The AA 2014 ingots were cut into several pieces and then were placed inside a stir casting furnace melting chamber. Before placing the ingots in the stir casting melting chamber, the inner wall of the melting chamber and the stirring blade with the shaft is evenly coated with a nano graphite paste to void interaction of the chamber liner and shaft material to diffuse into the final casted MMCs. AA 2014 ingot melting was performed using an induction electrical unit covering the melting chamber externally to a target temperature close to ∼750 °C. AA 2014 ingot initiated to melt around 610 °C while achieving a liquidus state at 640 °C. 10 g of magnesium powder was added as a wetting agent and stirring of the AA 2014 alloy melt was performed. The total stirring time was set to 20 min and the stirring revolution to 500 rpm respectively. Followed by stirring and successful creation of the whirlpool vortex of molten aluminium, the novel 2D – Gr$_{np}$ with 0.5 wt% (5 g) and AA 2014 powder (20 g) mixture was added to the molten pool and further stirred for 10 min.

The entire stirring process was carried out in a flushing argon atmosphere (2 Liters/min) through a zinc oxide-coated steel tube inside the melt chamber and which was well covered from top. Novel mixture addition is simultaneously coupled with 120 s of ultrasonication which facilitates temperature and particulate
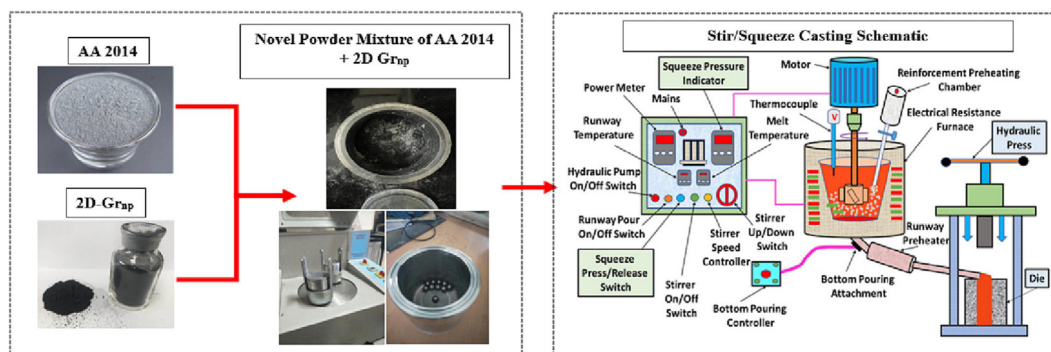

Fig. 1. Schematic of the novel mixture processing and the 2D – Gr$_{np}$/AA 2014 MMC using Squeeze casting process.
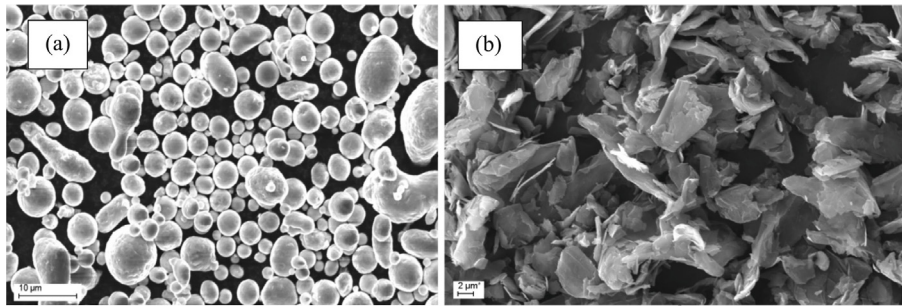
Fig. 2. FESEM of the as procured (a) aluminium alloy 2014 powder and (b) the 2D – Gr_{np} flakes.

Table 1
Elemental composition of AA 2014 as received from Ampal Inc. USA.

Type and element in wt. %	Al	Cu	Mg	Mn	Fe	Si
Powder	93.05 %	4.29 %	0.51 %	0.83 %	0.41 %	0.91 %
Ingot	92.85 %	4.26 %	0.65 %	0.79 %	0.57 %	0.88 %

homogenization in the melt chamber, which is found in other research works [24–26]. 2D – Gr_{np} nano particulate reinforced AA 2014 MMCs have been fabricated by introducing the synthesised powder mixture with embedded and interlocked 2D – Gr_{np} between the deformed AA 2014 particles. Post to the stirring and ultrasonication of the molten MMC pool, the novel mixture with deformed AA 2014 with embedded and interlocked 2D – Gr_{np} particles starts at to attain a semisolid state at 750 °C without losing its protective thin layer of aluminium oxide that prevents agglomeration or instant solidification of multiple reinforcing particles at single location.

The prepared molten melt was poured into a split mould made of D2 Steel designed and fabricated using ASTM B686/B686M standard for casting aluminium-based material. The pouring temperature of the molten MMC slurry was maintained at 650 °C. The D2 steel spilt mould was also preheated and maintained at 450 oC to avoid rapid cooling and prevent instant solidification of the MMC melt inside the die. Post to the pouring process very few materials slag is left in the stirring chamber and XRD study revealed that negligible amount of 2D – Gr_{np} is found and mostly the slag contained aluminium oxide particulates.

The overall dimension of the steel mould is 200 mm of height and 30 mm in diameter. Followed by the down pouring of the MMC melt into the die, a hydraulic unit with a ram is used to squeeze press the poured MMC melt with a compaction pressure of 110 MPa. The squeeze casted samples are naturally cooled and further heat treated using T6 standards with solution treated at 460 °C for 6 h and water quenched. Further the artificial aging was carried out on the MMC samples at 190 °C and furnace cooled to further test it for various mechanical and microstructural evaluations. Samples for testing were cut using a wire electric discharge machine (WEDM) to avoid the induced thermal residual stress during the sample preparation. Microstructural characterization was carried out using an optical inverted microscope (Dewinter – Dmi premium) and detailed characterization was also carried out using a field emission scanning electron microscope (FESEM Quanta 200 FEG) that is equipped with an energy dispersive x-ray spectroscopy (EDS) and element mapping facility. The samples for the microstructural characterization using FESEM and optical microscope were prepared by a mechanical grinding technique followed by a fine electrolytic polishing. Along with this High-Resolution Transmission Electron Microscopy (HRTEM) was carried out on the MMC samples using a FEI Tecnai TF20 HRTEM machine that operates at 200 KV FEG.

Precision Ion polishing system (PIPS) was used to synthesis the MMC samples for analysing in HRTEM observation. Further, the polished surface is applied and rinsed with Keller's reagent with chemical composition (2.5 ml HF, 3 ml HCl, 4.5 ml HNO_3 and 190 ml of H_2O) to etch the surface of the samples to observe the grain boundaries clearly. Crystallographic characterization of the casted MMC is also carried out using an electron backscattered diffraction (EBSD) method available and equipped in the FESEM used earlier. The average grain size and the crystal misorientation was recorded for the MMC by following the ASTM: E112 standard. Wide angle X-ray diffraction using XRD-Bruker D8 Advance was used to perform the phase analysis on the novel powder mixture, Squeeze casted MMC and the furnace residue post to the process of casting.

XRD rig equipped with Rigaku D/max diffractometer with CuKα with specific wavelength of 1.5406 Å and a high-speed energy dispersive detector (LYNXEYE XE-T) was used to analyse the MMC samples. Laser Raman spectroscopy (Renishaw, 532 nm Ar$^+$ sourced laser) was used to investigate the nature and quality of the 2D – Gr_{np} nanoparticulate. Tensile testing was performed using ASTM E 08 standard in an Instron – 8801 testing machine with maximum load capacity of 100 kN and test at strain rate of 0.5 mm/min. Microhardness measurements were carried out on the casted MMC plate using ASTM E18 standards using 1/16 mm steel ball with 100 KgF and a hardness map was developed throughout the MMC to understand the homogeneity of the novel mixture in the casted MMC. Fig. 3 represents the schematic of the location where the testing and analysis is carried out for the Squeeze casted 2D – Gr_{np} nano particulate reinforced AA 2014 MMC sample.

3. Results and discussion

3.1. Particle mechanics and characterization of synthesized 2D – Gr_{np}/ AA 2014 novel mixture

Initially, low energy (low speed) ball milling (LEBM) was carried out to synthesis the novel mixture of adding 2D – Gr_{np} into the AA 2014. Fig. 4a represents the FESEM image of the novel powder morphology and the particle mechanics at the start of the synthesis using LEBM (150 rpm 2 h). During this stage of LESM, the AA 2014 particles were observed to possess an undeformed spherical shape with few surface shear marks due to the generation of mild shear
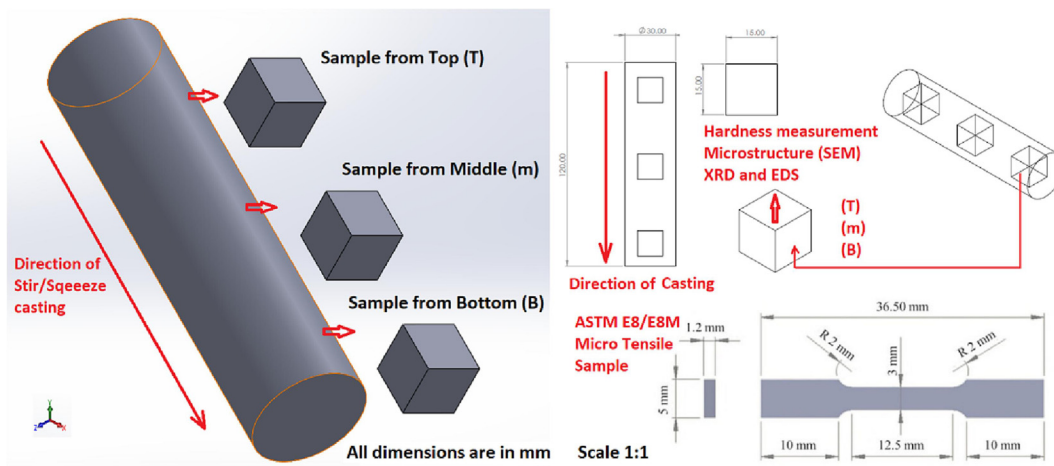
Fig. 3. Schematics of the places where the testing and characterization is carried out for the as-casted and T6 Treated MMC.
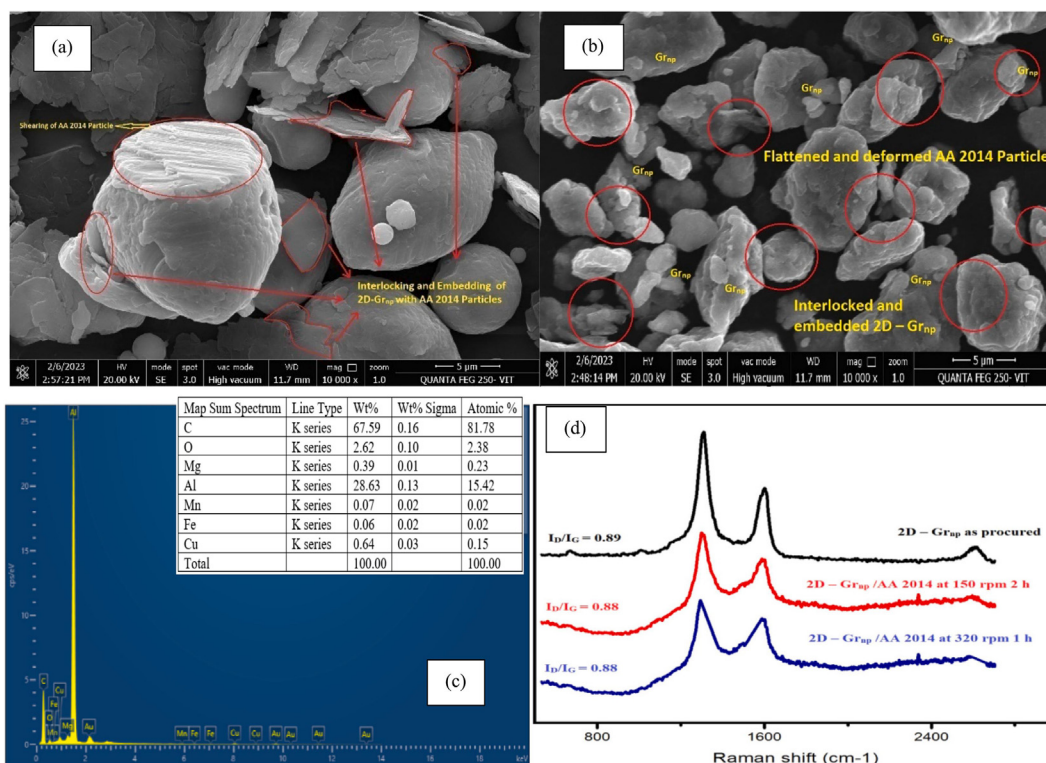

Fig. 4. FESEM of **a.** low revolution speed of 150 rpm for 2 h, **b.** high revolution speed of 320 rpm for 1 h, **c,** and **d.** EDS and Raman Spectrum of the synthesized 2D – Gr_{np}/AA 2014 novel mixture.

force from the colliding tungsten carbide balls. Along with the minimal surface shear marks, added 2D – Gr_{np} starts to integrate with the AA 2014 particle surface in two distinct mechanisms like interlocking between the AA 2014 particulates and embedding to the surface of the AA 2014 particulates which is clear evident from Fig. 4a and is consistent with the research finding [23–24]. Post to LEBM, High energy (high speed – 320 rpm 1 h) ball milling (HEBM) led to the generation of strong shear force due to the increase in tungsten carbide balls collision [31]. Deformation of the AA 2014 particulate from spherical shape to flat shape is observed with embedded and interlocked 2D – Gr_{np} on the surface and in between the particulates at the end of the process by synthesizing a novel powder mixture that can be used in reinforce-

ment material during Squeeze casting the homogeneously dispersed AA2014-2D – Gr_{np} MMC.

It is also evident that no trace of folded or wrinkled nature of 2D – Gr_{np} is observed from the interlocked and embedded 2D – Gr_{np} to the flattened AA 2014 particulates at the end of the HEPBM process. Various other materials research has proven that the HEPBM process plays a significant role in achieving homogeneous dispersion in the final MMC fabricated [25–27]. Fabricating this novel powder mixture by using HEPBM facilitates enhanced homogeneous dispersion and reduces agglomeration of 2D – Gr_{np} during the Squeeze casting process [28]. The interlocking and embedding mechanism reduces the agglomeration of 2D – Gr_{np} and is mostly avoided because of the flattened AA 2014 acting as a spacer

between the 2D – Gr_{np} layers. A detailed study using Raman spectroscopy was carried out on the as-procured 2D – Gr_{np}, novel mixture processed with LEBM and HEBM that provides information on the structural damage done to the 2D – Gr_{np} after the process of HEPBM [26]. From the Fig. 4d, the calculated I_D/I_G ratios are 0.89 and 0.88 respectively which is consistent with the other research findings [27]. The negligible variation in the calculated I_D/I_G ratio confirms the phenomenon of no damage is incurred to the 2D – Gr_{np} during the synthesis of the novel mixture using HEPBM technique.

3.2. Densification and microstructural characterisation of the MMC

The AA 2014/2D – Gr_{np} Squeeze casted MMC is fabricated by adding the novel mixture (2D – Gr_{np} with 0.5 wt% (5 g) and AA 2014 powder (20 g)) into the melt pool using AA 2014 ingots with 99.5% purity. The microstructural and strength properties were recorded in three different locations of the squeeze-casted MMC, as presented in Fig. 3. It is evident that the direct addition of 2D – Gr_{np} to the molten melt is difficult and causes 2D – Gr_{np} floating, non-homogeneous mixing and agglomeration [8]. By adding the novel mixture of HEPBM processed 2D – Gr_{np}/AA 2014 powder to the molten melt facilitated the process of homogeneous mixing of the added reinforcement in the molten melt by two key phenomena. During the addition of the novel mixture into the AA 2014 melt pool, dissolution of the AA 2014 powder interlocked and embedded with 2D – Gr_{np} occurs, which transfers the 2D – Gr_{np} throughout the molten melt pool, acting as an effective carrier

to facilitate the homogeneous dispersion of the 2D – Gr_{np} [21]. Dissolution of the AA 2014 also protects the interlocked and embedded with 2D – Gr_{np} from contact and reacting with the AA 2014 molten melt. Post to the addition of the novel mixture to the melt pool, the high-speed stirring at 500 rpm for 20 mins prevents the agglomeration of the 2D – Gr_{np} and from being sintered. It is also observed that using the AA 2014 particle that matches the density of the molten melt facilitates homogeneous movement and dispersion of the interlocked and embedded with 2D – Gr_{np} during the high-speed stirring at around 750 °C [34].

Fig. 5(a) represents the influence of 0.5 wt% 2D – Gr_{np} addition and the average grain size measured at the different locations of the Squeeze-casted MMC compared with the unreinforced AA 2014 alloy. It is clearly evident that 0.5 wt% 2D – Gr_{np} addition facilitated effective grain refinement, and it's been observed throughout the cast. The average grain observed after the addition of 0.5 wt% 2D – Gr_{np} was recorded to be 68 μm. This grain refinement of the AA 2014 α-aluminium grains from 540 μm to 68 μm is mainly due to the homogeneous dispersion of the added 2D – Gr_{np} [27]. The principal mechanism behind this aspect of grain refinement is that the homogeneously dispersed 2D – Gr_{np} acting as a nucleating spot during the solidification of the α- AA 2014 grains. Novel AA 2014 powder mixture with embedded and interlocked 2D – Gr_{np} during solidification pin to the grain boundaries and accelerate the grain refinement which tends to facilitate fine grain formation that deflects cracks and leading to increase in the mechanical properties of the fabricated MMCs [33–34]. It is consistent with other research that adding more than 0.5 wt% of 2D –
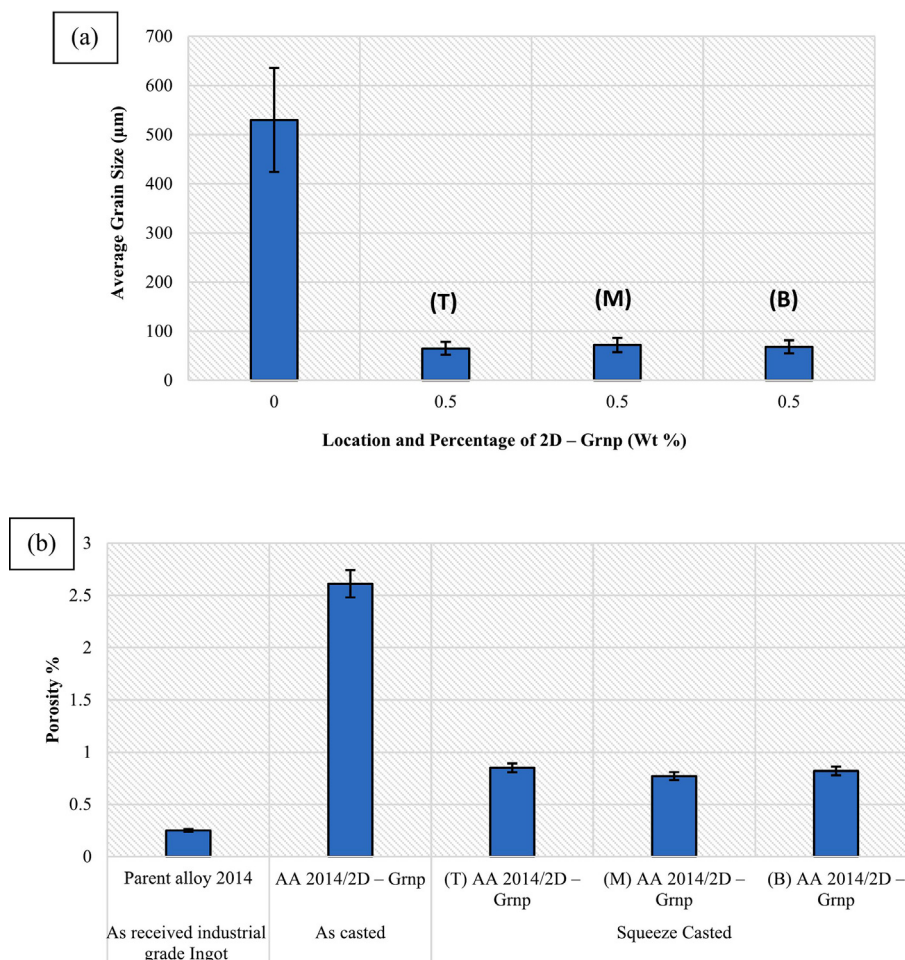

Fig. 5. (a) Average Grain size and **(b)** porosity % at various locations of AA 2014 reinforced with 0.5 wt% 2D – Gr_{np} along the direction of the Squeeze casting.

Table 2

Theoretical and Experimental Density of the pure alloy 2014, as casted and the squeeze casted MMC.

S.No.	Casting Type	Sample Description	Theoretical Density in g/cm³	Experimental Density in g/cm³	% Error
1	As received	Parent alloy 2014	2.765	2.771	0.21
2	As casted	AA 2014/2D – Gr_{np}	2.613	2.618	0.19
3	Squeeze Casted	(T) AA 2014/2D – Gr_{np}	2.678	2.669	0.32
4		(M) AA 2014/2D – Gr_{np}	2.673	2.666	0.25
5		(B) AA 2014/2D – Gr_{np}	2.675	2.668	0.25

Gr_{np} had a declining trend in the mechanical properties of the MMCs as there was no evidence of grain size reduction or grain refinement noticed in higher 2D – Gr_{np} amounts >0.5 wt% [29–31].

This characteristic behavior of grain refinement and improved MMC property is in good agreement with the density data presented in Table 2 and porosity % data presented in Fig. 5(b). Theoretical density of the developed MMC is calculated based on the rule of mixture principle as shown in Eq. (1), where ρ_{mmc}, ρ_{AA} and ρ_{Grnp} are the density of the MMC fabricated, AA 2014 and 2D – Gr_{np}. m is the mass of the AA 2014 and 2D – Gr_{np} used in this study. ASTM standard B962-17 is used to measure the experimental density of the fabricated MMC using Archimedes principle. The average of three measurements and calculations were considered in this validation [28].

$$\rho_{mmc} = \frac{1}{\frac{m_{AA}}{\rho_{AA}} + \frac{m_{Grnp}}{\rho_{Grnp}}} (g/cm^3) \tag{1}$$

The porosity percentage of the developed MMC before squeeze casting and after squeeze is calculated using the difference between the calculated theoretical density and the measured experimental density recorded in Table 2. From Table 2 it is evident that MMC processed by squeeze casting technique resulted in lower theoretical and experimental density compared to the parent alloy 2014. This phenomenon is mainly due to the homogeneous dispersion and addition of the novel powder mixture with embedded and interlocked 2D – Gr_{np} particulates [6,26]. However, there was an increase in theoretical and experimental density observed than the as casted MMC sample clearly confirms that 110 MPa of compaction pressure during the squeeze casting process facilitated in closing the fabrication defects like micropores, voids and microcracks [26].

The result of the porosity % calculation in Fig. 5(b) shows that industrial-procured AA 2014 ingot exhibited lowest porosity volume % of 0.25%. This means that industrial grade AA 2014 ingot was vacuum casted which exhibited the lowest porosity %. It is also clearly evident from Fig. 5(b) that stir casted MMC with 0.5 wt% 2D – Gr_{np} reinforced MMC exhibited the highest porosity volume % of 2.6%, which is ascribed to the formation of general defects like micropores, macro pores, voids and micro/macro cracks and defects that can be observed in a gravity casting process [8]. However, there was a decrease in porosity volume % from 2.6% to an average of 0.85 % in all the regions (T, M, B) observed than the as casted MMC sample clearly confirms that 110 MPa of compaction pressure during the squeeze casting process facilitated in closing the fabrication defects like micropores, voids and microcracks [8,26]. The porosity decrease was recorded to be by the factor of 67% which, is in good agreement with the research carried out with the same alloy matrix [26]. In various other researches, it is also reported that higher wt% (>0.5 wt%) of graphene content led to an increase in porosity and casting defects and eventually lower density and lower mechanical properties [8,26].

Fig. 6 shows the FESEM micrographs of the AA 2014 ingot as procured, and the novel mixture added AA 2014/0.5 wt% of 2D –

Gr_{np} MMC post to the T6 treatment after Squeeze-casted process. Comparing the FESEM micrographs of the pure AA 2014 ingot and the novel mixture reinforced MMC, it is evident that the novel mixture with embedded and interlocked 2D – Gr_{np} has significantly changed the dendritic grain morphology of the AA 2014 after the Squeeze casting process. This significant change in the grain morphology is observed identically in all places of the MMC cast, as clearly seen from Fig. 6(b – d) and is consistent with various research findings [6,16,18,20]. The microstructure throughout the MMC revealed that the addition of 2D – Gr_{np} resulted in the formation of the rosette-like microstructure which is highlighted with yellow circles in Fig. 6(b – d). MMC cast with rosette-like microstructure consists of the solid solution α-Al grain surrounded by the interdendritic secondary phases along with the finely dispersed novel mixture embedded and interlocked with 2D – Gr_{np}. In comparison with the casted MMC microstructure the AA 2014 ingot exhibit a courser microstructure with average grain size of 540 μm.

From Fig. 6(b – d) it is evident that a novel mixture with embedded and interlocked 2D – Gr_{np} along with a higher stirring speed of 500 rpm for 20 mins resulted in an increase in the number of fine grain boundaries which also facilitated in an increase in more homogeneous nucleation of the intermetallic precipitates that are highlighted with the red circles in the enlarged micrographs. 0.5 wt% of 2D – Gr_{np} was found optimal and effective to fabricate the AA 2014/2D – Gr_{np} MMC and is consistent with the findings reported by other research works [23,25–27]. XRD analysis was carried out for the phase identification of the pure ingot AA 2014, the novel mixture (powder AA 2014/2D – Gr_{np}), and at three locations (T, M, B) for the T6 treated Squeeze casted MMC as shown in Fig. 7. The XRD peak proves the presence of the α-Al in the casted MMC as the major matrix element. The presence and nature of the AA 2014/2D – Gr_{np} novel powder mixture with embedded and interlocked 2D – Gr_{np} were observed at all three locations (T, M, B) of the casted MMC and there was no trace of aluminium carbide (Al_4C_3) formation were observed in the final MMC fabricated [32].

Fig. 8 shows the FESEM micrograph of the enlarged grain boundary of the casted MMC reinforced with a novel powder mixture with embedded and interlocked 2D – Gr_{np}. From Fig. 6(b – d) it is evident that the novel powder mixture was homogeneously dispersed in the final MMC cast. Homogeneously dispersed novel mixture with embedded and interlocked 2D – Gr_{np} and squeeze casting process facilitated in the formation of the fine equiaxed grains with the fine dendritic structure throughout the MMC cast which is in good agreement with the density data furnished in Table 2. In overall the microstructure throughout the cast consisted of the fine spherical-shaped grains and fine equiaxed grains with a clear presence of the embedded and interlocked 2D – Gr_{np} and the intermetallic precipitates at the grain boundaries and in the matrix itself [28].

Compared with the different locations of the MMC cast, the microstructure at the top, middle and bottom exhibited uniform dendritic cells with finer spherical grains, and moreover, the fine
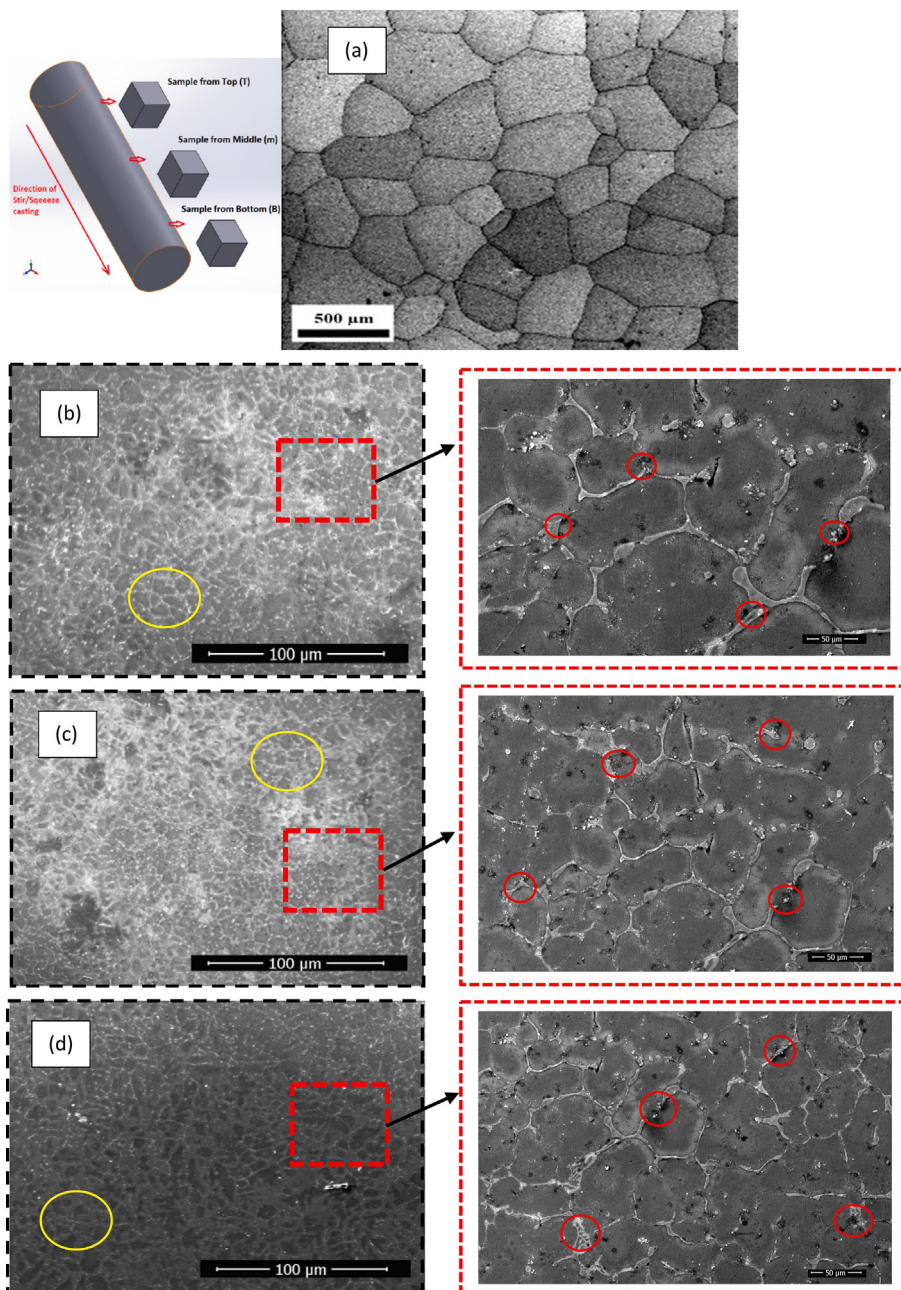
Fig. 6. FESEM microstructure of AA 2014, with (a) ingot in as procured condition, location of the MMC cast (b) Top (T), (c) Middle (M) and (d) bottom (B) of the AA 2014/novel mixture (AA 2014/0.5 wt. %2D – Gr$_{np}$) reinforced MMC treated for T6 condition.

spherical grains are observed throughout the MMC cast [23–27]. This phenomenon of formation of fine spherical grains are strongly owing to the compaction pressure at which the squeeze casting is performed (110 MPa). Under the squeezing load, the grains and the bulk solidify rapidly, which arrests the further grain growth of the α-AA 2014 grains. It is also evident from the EDS analysis of the casted MMC that the presence of the equilibrium phase θ-Al$_2$Cu intermetallic, which matches the copper and carbon levels and observed to be higher than the average wt % of the chemical composition in the parent alloy. This equilibrium phase θ-Al$_2$Cu intermetallic forms by dissolving two atoms of aluminium, one atom of copper and two more by vacancies and its mostly observed in the grain boundaries, inside the α-AA 2014 grains and the interfaces of the novel mixture-AA 2014 and was homogeneously nucleated [29].

3.3. Solidification mechanism of the novel mixture (2D – Gr$_{np}$/AA 2014) reinforced MMC

Novel mixture addition facilitated the homogeneous dispersion of 2D – Gr$_{np}$ into the molten metal that did facilitate homogeneous nucleation of the equilibrium phase θ-Al$_2$Cu and grain boundary refinement post to the casting process. As a result of the homogeneous dispersion of the Novel mixture with embedded and interlocked 2D – Gr$_{np}$ led to three significant phenomena of particulate strengthening, effective grain refinement and precipitation strengthening of the developed MMC [33].

The uniformly dispersed novel mixture with embedded and interlocked 2D – Gr$_{np}$ acted as the start point of the grain/precipitate nucleation and end point of the grain/precipitate growth, which is clearly seen in Fig. 9a with red boundaries with dispersed
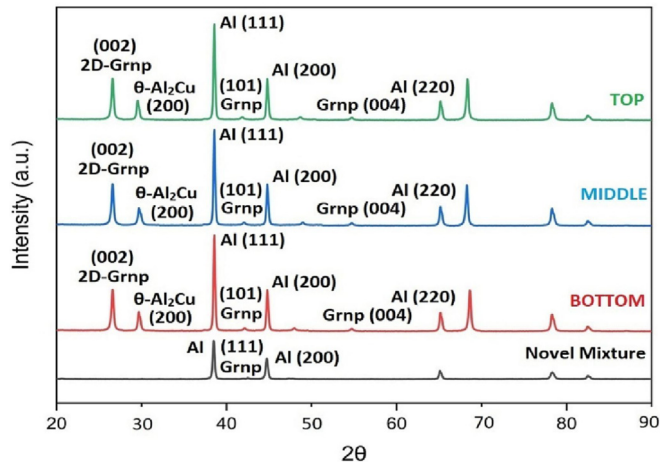
Fig. 7. XRD pattern of (a) pure ingot AA 2014, (b) the novel mixture (powder AA 2014/2D – Grnp) and (c) at three locations (T, M, B) for the T6 treated Squeeze casted MMC.

2D – Gr$_{np}$ inside the α-AA2014 grains. The formation of the equilibrium phase θ-Al$_2$Cu and the grain boundary refinement is achieved due to the slower cooling or heating at higher process temperatures. Being homogeneous and coherent, it contributes well to the hardening of the MMCs developed using the Squeeze casting technique. Additionally, there have been three class of mechanism models that are proven related to the homogeneous dispersion of the particulate into a matrix metal, namely (1) kinetic models that predict the solid/liquid interface velocity, which is critical due to the transition from novel α-AA 2014 powder particle with embedded and interlocked 2D – Gr$_{np}$ pushing to engulfment, (2) thermodynamic models [27] related to the conventional heterogeneous nucleation model and (3) models using the ratio between the thermomechanical properties of the novel powder mixture with embedded and interlocked 2D – Gr$_{np}$ and the 2014 melt [23,25].

The first model predicts the dispersion capability in common which relates to the dependency of the added reinforcement dispersion behavior on the processing boundaries. The last two models exhibit that the thermal conductivity of the added reinforcement particulate into the molten metal that relates to

the switch of the interface structure from convex to concave as the added novel mixture with embedded and interlocked 2D – Gr$_{np}$ does influence the solidification mechanics of the 2014 matrix metal [26–28].

This phenomenon of achieving homogeneous dispersion of the reinforced novel mixture with embedded and interlocked 2D – Gr$_{np}$ significantly affected the temperature gradient during the solidification in the entire MMC cast. During the solidification homogeneously dispersed novel mixture with embedded and interlocked 2D – Gr$_{np}$ facilitated the rapid heat removal that will be utilized for further solidification and prevents α-Aa 2014 grain growth. It is well known that homogeneously dispersed novel mixtures with embedded and interlocked 2D – Gr$_{np}$ possess high thermal conductivity, which facilitated in removing excess heat and achieving homogeneously fine spherical shaped grains and fine equiaxed grains with clear presence of the embedded and interlocked 2D – Gr$_{np}$ and the intermetallic precipitates at the grain boundaries and in the matrix itself throughout the MMC cast in all locations (T, M, B) which is evident from Fig. 6(b – d), Fig. 8 and Fig. 9a.

3.4. Rockwell hardness analysis

Fig. 10 shows (a) the schematic of the measuring locations and (b) the Rockwell hardness results of the Squeeze casted MMC fabricated by reinforcing with synthesized novel powder mixture (2D – Gr$_{np}$/AA 2014) at three different locations (T, M, B). At all the samples from three individual locations, the hardness measurement readings were recorded in a 5x5 array matrix with 2.5 mm of offset between the measurements. ASTM E 18 standard was used to measure the Rockwell hardness on the sample surface by following the parameters as discussed earlier. Fig. 10(b) provides the average values of 25 readings from each location (T, M, B) and compared with the unreinforced parent alloy. It is evident from the Fig. 10(b) that there is an increase in the hardness values by the addition of the novel powder mixture with embedded and interlocked 2D – Gr$_{np}$ from 82 HRB (Parent alloy) to an average of 101 HRB in as casted condition and to 119 HRB in T6 condition irrespective of the location measured. Hardness values from all the locations were recorded the same and it is found to increase by 23 % for as-casted condition and 45.5 % increase for the T6 condition from the parent alloy.
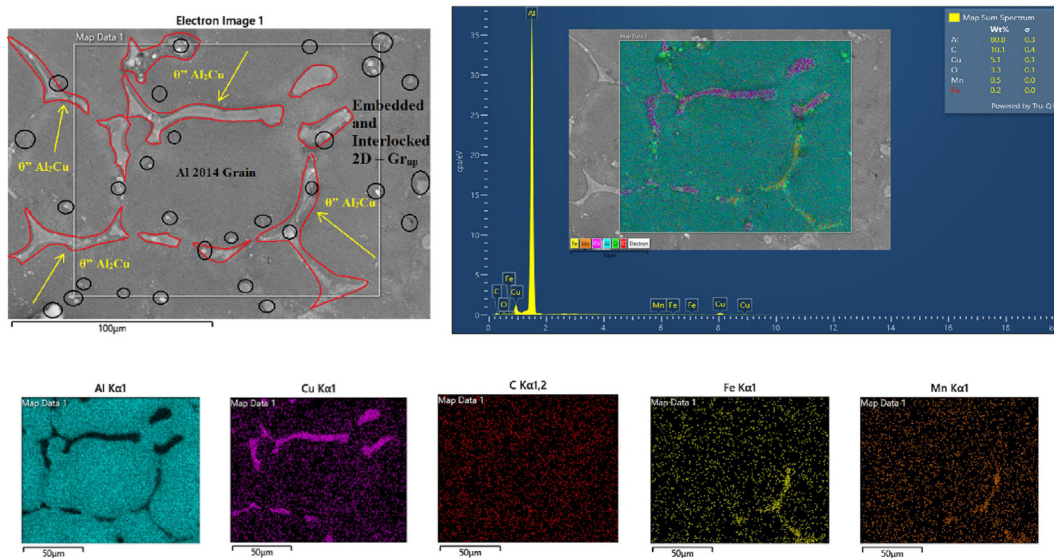

Fig. 8. FESEM of the enlarged grain boundary with element mapping and EDS analysis of the eutectic phase in T6 treated MMC cast.
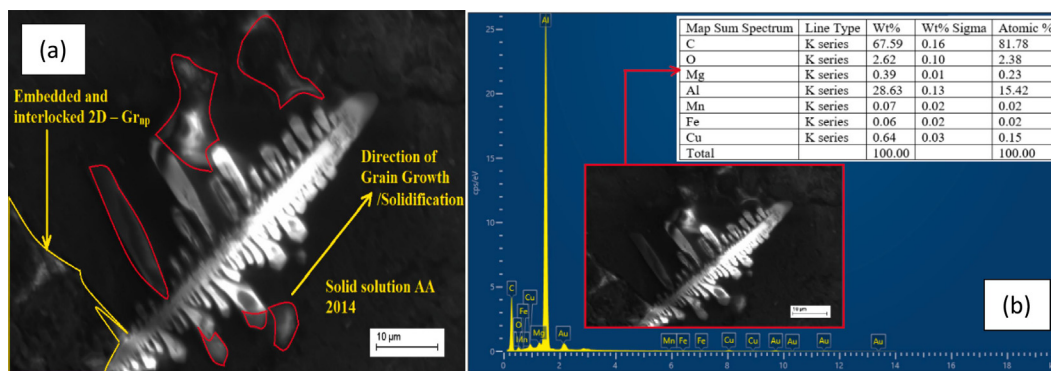
Fig. 9. FESEM micrographs of the T6 treated MMC samples showing the influence of Novel mixture (2D – Gr$_{np}$/AA 2014) addition on the Solidification mechanics.
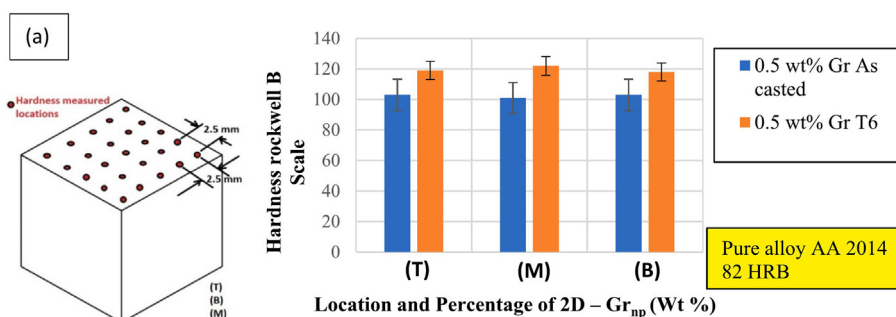

Fig. 10. Rockwell Hardness of (a) Schematic and (b) Novel Mixture reinforced (2D – Gr$_{np}$/AA 2014) AA 2014-2D – Gr$_{np}$ MMC measured at different location (T, M, B) in the T6 treated MMC cast.

This phenomenon of uniform hardness in all locations is attributed to the fact of achieving homogeneous dispersion of 2D – Gr$_{np}$ by using the novel powder mixture with embedded and interlocked 2D – Gr$_{np}$ along with the improved density and reduced porosity, which is evident and supported by the FESEM morphology and XRD data presented in Fig. 5(b), 6 and 7. Three major strengthening mechanisms are responsible for the enhancement in the hardness recording were (1) precipitation hardening because of the homogeneous nucleation of stable θ-Al$_2$Cu, (2) grain refinement strengthening influenced by the homogeneous dispersion of the novel powder mixture with embedded and interlocked 2D – Gr$_{np}$ and (3) dispersion strengthening of the novel powder mixture with embedded and interlocked 2D – Gr$_{np}$. MMC reinforced with a novel mixture with embedded and interlocked 2D – Gr$_{np}$ and the above confirmed strengthening mechanism are verified with the HRTEM characterization carried out at the three locations (T, M, B) of the Squeeze MMC as shown in the Figure (a), (b) and (c). Homogeneously dispersed novel powder mixture with embedded and interlocked 2D – Gr$_{np}$ facilitated homogeneous nucleation of the stable equilibrium phase θ-Al$_2$Cu, and upon squeeze casting, the aluminium α-AA 2014 grain becomes soft to accommodate and implant the nucleated and dispersed novel powder mixture with embedded and interlocked 2D – Gr$_{np}$ and ends up in formation of the finer grain boundary as clearly seen in all section (T, M, B) of the T6 treated MMC cast [32].

3.5. Tensile behavior

Fig. 12 represents the comparison of the ultimate tensile strength (UTS) data of the T6 treated and as-cast 0.5 wt% 2D – Gr$_{np}$/AA 2014 MMC. The data were acquired by using a micro tensile specimen for metal and MMCs, and the sample dimensions are provided in Fig. 3 and are measured in all three locations (T, M,

B) and the reported values are average of three trails per location. It is found from the graph provided in Fig. 12(a) that addition of 0.5 wt% 2D – Gr$_{np}$ and homogeneous dispersion of the novel powder mixture with embedded and interlocked 2D – Gr$_{np}$ and fabrication of defect-free and highly dense MMC by squeeze casting process significantly influenced the increase in the UTS values from 185 MPa (Pure alloy) to 310 MPa (MMC as casted condition with the presence of homogeneously dispersed 2D – Gr$_{np}$) which is observed to exhibit 67% increase from the as casted condition [26,33]. Further increase in UTS by 32% (from 310 to 360 MPa) is found in the final MMC cast processed with T6 heat treatment procedure.

0.5 wt% 2D – Gr$_{np}$ addition, squeeze casting and T6 heat treatment played a significant role in improving the final MMC plate properties and is in good agreement with other research carried out earlier [23–27]. Various researches proved that reinforcing with more than 0.5 wt% 2D – Gr$_{np}$ resulted in a decline trend of the mechanical properties and found that 0.5 wt% of 2D – Gr$_{np}$ addition is the threshold quantity to fabricate a superior MMC with aluminium as a matrix metal [23–27]. Improving the mechanical properties of any ductile material like aluminium is purely depending on the reinforcement type, shape, total weight percentage (wt. %), secondary processing like heat treatment and most importantly, achieving the homogeneous dispersion of the nano 2D – Gr$_{np}$ and engineering the nucleation mechanics of the intermetallics in the grain boundary and within the α-aluminium grain itself is highly significant [11].

The first primary mechanism of the strength increase is greatly due to the extensive grain refinement facilitated by the homogeneously dispersed novel mixture with embedded and interlocked 2D – Gr$_{np}$, which also further influenced the homogeneous nucleation of the stable θ-Al$_2$Cu at the grain boundary and in α-AA 2014 grain itself as evident from all the HRTEM micrographs pre-
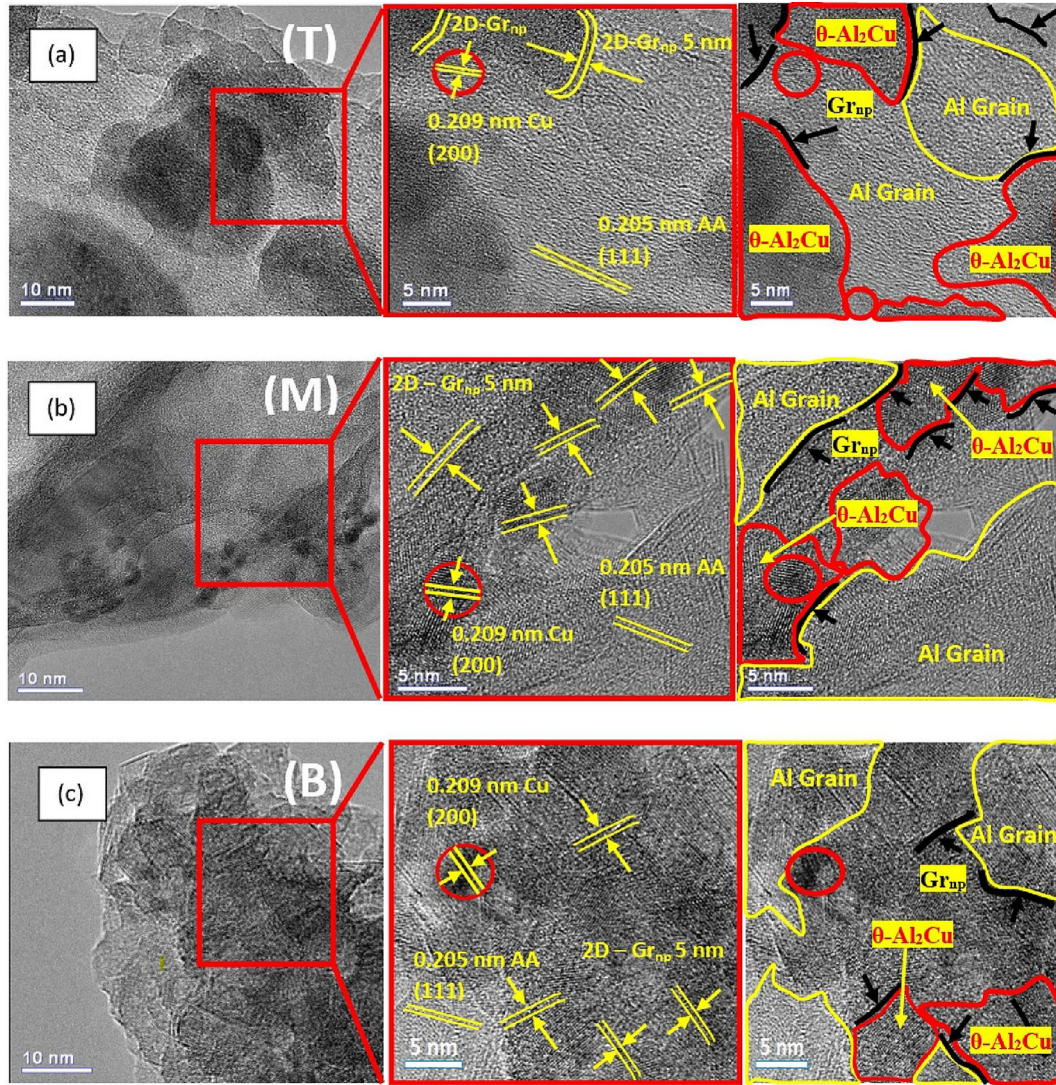
Fig. 11. HRTEM micrographs of the T6 treated 0.5 wt% 2D – Gr$_{np}$/AA 2014 MMC characterized after squeeze casting process (a) top of the MMC cast, (b) middle of the MMC cast and (c) bottom of the MMC cast as shown in the schematic provided in Fig. 3.

sented in Fig. 11(a – c). As evident from the HRTEM micrographs, the nucleation of the stable θ-Al$_2$Cu intermetallic precipitate is facilitated by the T6 heat treatment and from the solid solution of AA 2014 with Al-Cu through the Squeeze casting process. The key strengthening mechanism by Orowan strengthening mechanism is backing up this homogeneous nucleation of the stable θ-Al$_2$Cu intermetallic precipitate, which is presented in Eq. (2) and Eq. (3) [21].

$$\Delta\sigma_{Orowan} = MGb\frac{\sqrt{f}}{r} = MGb\frac{1}{L} \qquad (2)$$

$$L = \sqrt{\frac{2}{3}}D_p\left(\sqrt{\frac{\pi}{4f}} - 1\right) \qquad (3)$$

Where M is the mean orientation factor (3.06 for all FCC based metallic material), G is the modulus of shear (26 MPa for aluminium), b is the burgers vector value (0.286 nm for aluminium), L is the inter-particulate spacing, D$_p$ is the average particle diameter of the homogeneously dispersed novel powder mixture with embedded and interlocked 2D – Gr$_{np}$, f is the volume fraction of the nucleated stable θ-Al$_2$Cu intermetallic precipitate inside the

MMC cast. Another key strengthening mechanism that is responsible for the increase in the mechanical properties of the MMC cast according to hall-petch theory [36], which relates the grain size and the final mechanical properties, as evident from Fig. 12(b). This current research validated the grain refinement (Fig. 5) at all locations of the MMC cast (T, M, B) and it is proven that a novel mixture with embedded and interlocked 2D – Gr$_{np}$ produced finer grains and facilitated homogeneous nucleation of the stable θ-Al$_2$Cu intermetallic precipitate in the grain boundary, α-AA 2014-2D – Gr$_{np}$ interfaces and inside the α-AA 2014 itself which is evident and highlighted in the HRTEM micrographs provided in Fig. 11(a – c).

However, the strengthening mechanism of the AA 2014 matrix cannot be only influenced by the addition of 2D – Gr$_{np}$ alone, T6 treatment also played a significant role in improving the properties according to the precipitation mechanics observed from the HRTEM micrographs presented in Fig. 11(a – c). We can find thick (5 nm) multi-layers of the embedded and interlocked 2D – Gr$_{np}$ at the grain boundary as highlighted in Fig. 11(a – c) uniformly observed in all the locations of the MMC cast. It is well understood that homogeneously dispersed novel powder mixture with embedded and interlocked 2D – Gr$_{np}$ influenced the nucleation mechanics
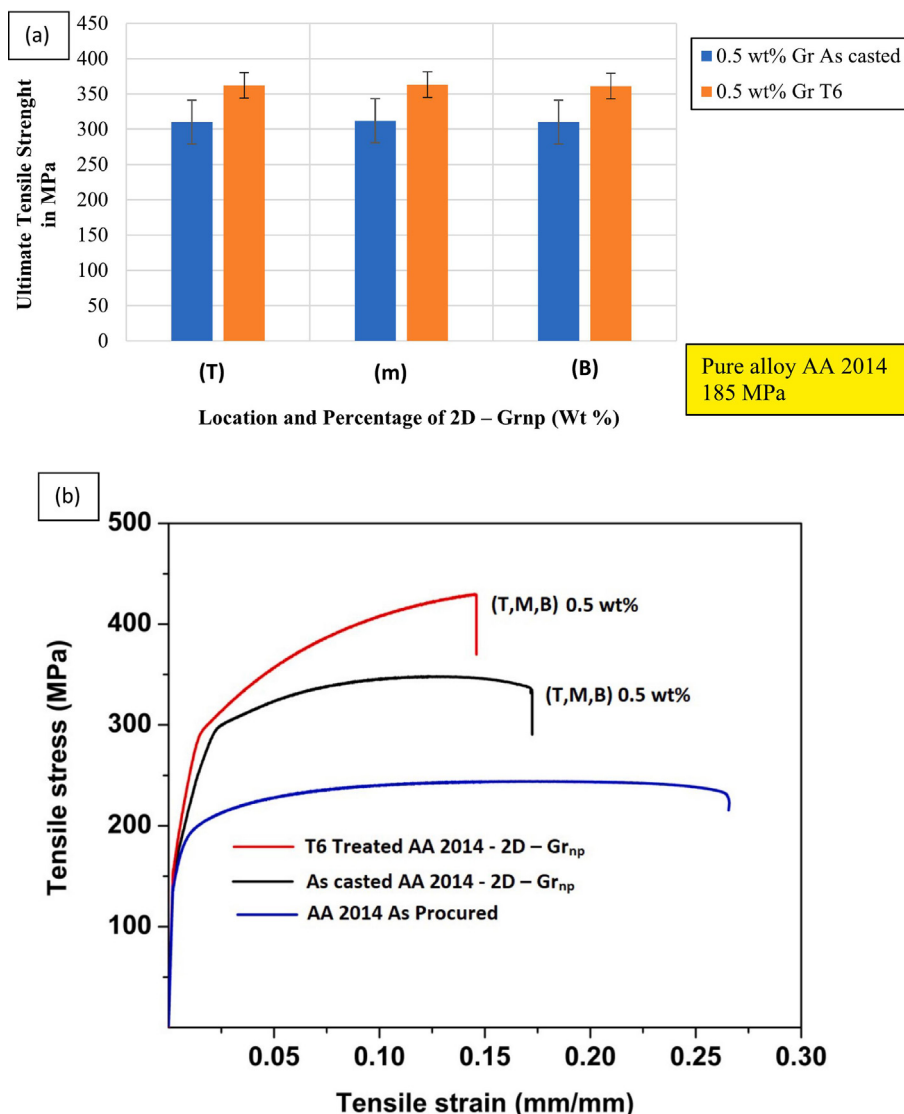
Fig. 12. Tensile stress vs. strain of the T6 treated 0.5 wt% 2D – Gr_{np}/AA 2014 Squeeze casted MMC.

of the stable θ-Al_2Cu intermetallic precipitate in the grain boundary, α-AA 2014-2D – Gr_{np} interfaces and inside the α-AA 2014 itself after Squeeze casting process and is in good agreement with the XRD patterns of the T6 processed specimens (Fig. 7).

It is very important to analyze the deformation behavior of the developed MMC and is validated using the tensile stress vs strain curve generated at all the locations, which was compared with the pure AA 2014 alloy. The UTS of AA 2014 alloy increased with the addition of the novel powder mixture with embedded and interlocked 2D – Gr_{np} and its homogeneous dispersion facilitated the increase at an expense of elongation to failure as seen clearly in Fig. 12(b). Looking at the strain-to-failure trend of them, a reduction in the strain-to-failure values was recorded in all locations (T, M, B) for as 0.5 wt% reinforced as-casted and T6 heat-treated MMC. This phenomenon of reduction in strain to failure is mainly due to the particulate strengthening mechanism caused by the homogeneously dispersed novel powder mixture with embedded and interlocked 2D – Gr_{np} which bends and bows the dislocation during the testing which led to lesser plastic deformation and improved strain hardening effect [37].

Specifically with the presence of homogeneously dispersed 0.5 wt% of 2D – Gr_{np}, homogeneously nucleated stable θ-Al_2Cu intermetallic precipitate in the grain boundary, α-AA 2014-2D – Gr_{np} interfaces and inside the α-AA 2014 itself, the plastic flow mechanics during the loading was transformed and localized deformation behavior of the α-AA 2014 grain was induced. Along with this the dislocations were pinned and getting blocked at the matrix-α-AA 2014-2D – Gr_{np}-θ-Al_2Cu interfaces during the loading condition which also resulted in MMC samples exhibiting reduced strain to failure of 40% (observed for MMC at as casted) and a strain to failure reduction of 44% (Observed for MMC at T6 condition) as seen from Fig. 12(b).

Fig. 13(a and b) clearly shows the failure mechanics of the MMCs to be a ductile mode failure with fine cup shaped dimples for 0.5 wt% 2D – Gr_{np} during the external loading. This study confirms the presence of homogeneously dispersed 0.5 wt% of 2D – Gr_{np}, homogeneously nucleated stable θ-Al_2Cu intermetallic precipitate in the grain boundary, α-AA 2014-2D – Gr_{np} interfaces and inside the α-AA 2014 itself that facilitated in improving the strength of the MMCs that includes mechanism like stress disper-
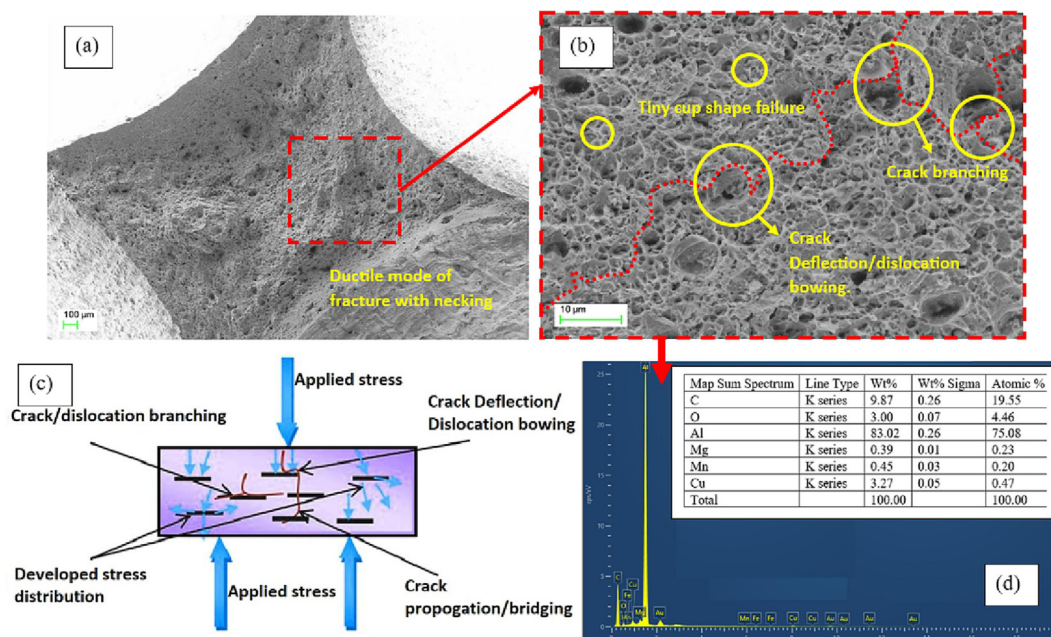
Fig. 13. (a) and (b) Fracture surface morphology of the T6 treated 0.5 wt% 2D – Gr$_{np}$/AA 2014 squeeze casted MMC (m) (c) the fracturing mechanics and (d) is the EDS spectrum of the fracture surface.

sion, crack deflection, linking and branching as seen from a schematic representation of the fracture surface (Fig. 13(b and c)) [30,33]. The crack branching or deflection led to the dislocation bowing mechanism that increased the path of crack propagation, which improved the mechanical strength of AA2014 matrix, as seen in Fig. 13(b) [30,33]. Likewise, through the crack bridging mechanism of homogeneously dispersed 2D – Gr$_{np}$ could absorb the excess loading energy efficiently during the application of external load [35–37]. The whole crack propagation mechanism is presented in the schematic provided in Fig. 13(c). The EDS data from the fracture surface confirms the presence of the 2D – Gr$_{np}$ and the copper based intermetallics with higher levels than usual (Fig. 13(d)).

The superior strength in the MMC is also due to the strong interfacial bonding between the α-AA 2014 grain achieved by squeeze casting process and the homogeneously dispersed 0.5 wt % of 2D – Gr$_{np}$ which increased the load transfer efficiency that eliminates the obliteration of the stress concentration during the loading. In addition, homogeneously dispersed 0.5 wt% of 2D – Gr$_{np}$, homogeneously nucleated stable θ-Al$_2$Cu intermetallic precipitate in the grain boundary, α-AA 2014-2D – Gr$_{np}$ interfaces and inside the α-AA 2014 itself provided higher resistance to the crack propagation which led to dislocation bowing around the 2D – Gr$_{np}$-θ-Al$_2$Cu-α-AA 2014 interface that can be seen from Fig. 13 (b) [21–29,30].

4. Conclusions

In this study, an aluminium-copper based alloy system (AA 2014) and its MMCs were engineered using a novel powder mixture with embedded and interlocked 2D – Gr$_{np}$. The developed novel MMC was aimed at for launch vehicle Super Lightweight fuel Tank (SLWT) Structural Application which uses another aluminium copper system made of AA 2219 and AA 2195 with 1 wt% lithium [3]. However, the developed novel mixture with embedded and interlocked 2D – Gr$_{np}$ using their own parent alloy powder facili-

tated homogeneous dispersion in the final cast when fabricated through Squeeze casting process. The experimental findings are listed as follows.

1. Novel mixture with matrix of AA 2014 powder with embedded and interlocked 2D – Gr$_{np}$ clearly acted as an effective carrier of 2D – Gr$_{np}$ during the stirring process and resulted in homogeneous dispersion in the aluminium alloy 2014 matrix and throughout the MMC cast.
2. Homogeneous dispersion of the novel powder mixture with embedded and interlocked 2D – Gr$_{np}$ resulted in grain refinement and acted as a homogeneous nucleation site during the T6 heat treatment process that resulted in enhanced strength properties. (Rockwell hardness from 82 to 119 HRB and UTS from 185 to 360 MPa).
3. 0.5 wt% 2D – Gr$_{np}$ addition to AA 2014 matrix exhibited enhancement in the mechanical properties, including Rockwell hardness and UTS, which is in good agreement with the strengthening mechanism related to grain boundary/refinement strengthening, precipitation hardening and particulate strengthening mechanism.
4. From the FESEM and HRTEM characterization, homogeneous dispersion of the novel powder mixture and the 2D – Gr$_{np}$-θ-Al$_2$Cu-α-AA 2014 interface integrity is found to be improved and is uniformly observed in all the locations of the casted MMC (T, M, B).
5. HRTEM observation on the interfaces clearly proves that nucleation of the stable θ-Al$_2$Cu intermetallic precipitate is strongly influenced by the homogeneously dispersed novel mixture with embedded and interlocked 2D – Gr$_{np}$ that led to improved mechanical properties of the final MMC cast.

In overall, this research facilitates in understanding the large-scale production of aluminium based MMC plate with homogeneous dispersion at large dimensions. As this research work focuses on finding an alternate super lightweight MMC materials and their effective fabrication route for the launch vehicle Super

Lightweight fuel Tank (SLWT) Structural Application, it is found that synthesizing novel powder mixture with same matrix material powder (same as the ingot material used for casting) facilitates homogeneous dispersion of the nano low dense reinforcements like 2D – Gr_{np} at optimal stirring parameters and Squeeze casting parameters.

Data availability

Data will be made available on request.

Declaration of Competing Interest

The authors declare that they have no known competing financial interests or personal relationships that could have appeared to influence the work reported in this paper.

References

[1] J. Hirsch, Aluminium in innovative light-weight car design, Materials transactions 52 (5) (2011) 818–824.

[2] T. Dursun, C. Soutis, Recent developments in advanced aircraft aluminium alloys, Materials & Design 1980–2015 (56) (2014) 862–871.

[3] A.K. Srivastava, B. Sharma, B.R. Saju, A. Shukla, A. Saxena, N.K. Maurya, Effect of Graphene nanoparticles on microstructural and mechanical properties of aluminum-based nano composites fabricated by stir casting, World Journal of Engineering 17 (6) (2020) 859–866.

[4] Rambabu, P.P.N.K.V., Eswara Prasad, N., Kutumbarao, V.V. and Wanhill, R.J.H., 2017. Aluminium alloys for aerospace applications. Aerospace Materials and Material Technologies: Volume 1: Aerospace Materials, pp.29-52.

[5] Kermanidis, A.T., 2020. Aircraft aluminum alloys: applications and future trends. Revolutionizing Aircraft Materials and Processes, pp.21-55.

[6] T. Arunkumar, V. Pavanan, V.A. Murugesan, V. Mohanavel, K. Ramachandran, Influence of nanoparticles reinforcements on aluminium 6061 alloys fabricated via novel ultrasonic aided rheo-squeeze casting method, Metals and Materials International 28 (1) (2022) 145–154.

[7] M. Alipour, R. Eslami-Farsani, Synthesis and characterization of graphene nanoplatelets reinforced AA7068 matrix nano composites produced by liquid metallurgy route, Materials Science and Engineering: A 706 (2017) 71–82.

[8] P.A. Rometsch, Y. Zhang, S. Knight, Heat treatment of 7xxx series aluminium alloys—Some recent developments, Transactions of Nonferrous Metals Society of China 24 (7) (2014) 2003–2017.

[9] A. Ramanathan, P.K. Krishnan, R. Muraliraja, A review on the production of metal matrix MMCs through stir casting–Furnace design, properties, challenges, and research opportunities, Journal of Manufacturing processes 42 (2019) 213–245.

[10] W. Chen, T. Yang, L. Dong, A. Elmasry, J. Song, N. Deng, A. Elmarakbi, T. Liu, H.B. Lv, Y.Q. Fu, Advances in graphene reinforced metal matrix nano Composites: Mechanisms, processing, modelling, properties, and applications, Nanotechnology and Precision Engineering 3 (4) (2020) 189–210.

[11] S.E. Shin, D.H. Bae, Deformation behavior of aluminum alloy matrix MMCs reinforced with few-layer graphene, MMCs Part A: Applied Science and Manufacturing 78 (2015) 42–47.

[12] S. Venkatesan, A. Xavior, Experimental investigation on stir and squeeze casted aluminum alloy MMCs reinforced with graphene, Materials Research Express 6 (12) (2019) 126542.

[13] V. Chak, H. Chattopadhyay, Fabrication and heat treatment of graphene nanoplatelets reinforced aluminium nano composites, Materials Science and Engineering: A 791 (2020) 139657.

[14] A.M. Ali, M.Z. Omar, H. Hashim, M.S. Salleh, I.F. Mohamed, Recent development in graphene-reinforced aluminium matrix MMC: A review, Reviews on Advanced Materials Science 60 (1) (2021) 801–817.

[15] M. Khan, R.U. Din, M.A. Basit, A. Wadood, S.W. Husain, S. Akhtar, R.E. Aune, Study of microstructure and mechanical behaviour of aluminium alloy hybrid MMC with boron carbide and graphene nanoplatelets, Materials Chemistry and Physics 271 (2021) 124936.

[16] B. Nayak, R.K. Sahu, Experimental and Digimat-FE based representative volume element analysis of exceptional graphene flakes/aluminium alloy nano composite characteristics, Materials Research Express 6 (11) (2019) 116593.

[17] I.G. Brodova, A.N. Petrova, I.G. Shirinkina, D.Y. Rasposienko, L.A. Yolshina, R.V. Muradymov, S.V. Razorenov, E.V. Shorokhov, Mechanical properties of sub microcrystalline aluminium matrix MMCs reinforced by "in situ" graphene through severe plastic deformation processes, Journal of Alloys and Compounds 859 (2021) 158387.

[18] A. Naseer, F. Ahmad, M. Aslam, B.H. Guan, W.S.W. Harun, N. Muhamad, M.R. Raza, R.M. German, A review of processing techniques for graphene-reinforced metal matrix composites, Materials and Manufacturing Processes 34 (9) (2019) 957–985.

[19] V. Khanna, V. Kumar, S.A. Bansal, Mechanical properties of aluminium-graphene/carbon nanotubes (CNTs) metal matrix MMCs: Advancement, opportunities, and perspective, Materials Research Bulletin 138 (2021) 111224.

[20] X. Wen, R. Joshi, 2D materials-based metal matrix MMCs, Journal of Physics D: Applied Physics 53 (42) (2020) 423001.

[21] M. Naik H R, M. L h, V. Malik, M. Patel GC, K.K. Saxena, A. Lakshmikanthan, Effect of microstructure, mechanical and wear on Al-CNTs/graphene hybrid MMC'S, Advances in Materials and Processing Technologies 8 (sup2) (2022) 366–379.

[22] Shil, A., Roy, S., Balaji, P.S., Katiyar, J.K., Pramanik, S., and Sharma, A.K., 2019, November. Experimental analysis of mechanical properties of stir casted aluminium-graphene nano composites. In IOP Conference Series: Materials Science and Engineering (Vol. 653, No. 1, p. 012021). IOP Publishing.

[23] Z. Zheng, X. Zhang, J. Li, L. Geng, Achieving homogeneous distribution of high-content graphene in aluminum alloys via high-temperature cumulative shear deformation, Materials & Design 193 (2020) 108796.

[24] J. Su, J. Teng, Recent progress in graphene-reinforced aluminum matrix composites, Frontiers of Materials Science 15 (1) (2021) 79–97.

[25] L.D. Kumar, S.S. Kulkarni, J.N. Deepu, N. Subramani, K. Sivaprakash, Investigation of mechanical & corrosion properties of graphene, R-glass fiber reinforced Aluminium 2024 hybrid MMCs, Materials Today: Proceedings 43 (2021) 1684–1693.

[26] X. Han, L. Yang, N. Zhao, C. He, Copper-Coated Graphene Nanoplatelets-Reinforced Al–Si Alloy Matrix MMCs Fabricated by Stir Casting Method, Acta Metallurgica Sinica (English Letters) 34 (2021) 111–124.

[27] P. Ashwath, P. Jeyapandiarajan, J. Joel, M.A. Xavior, N. Sumanth, C.S. Reddy, Flexural studies of graphene reinforced aluminium metal matrix MMC, Materials Today: Proceedings 5 (5) (2018) 13459–13463.

[28] J. Jayaseelan, A. Pazhani, A.X. Michael, J. Paulchamy, A. Batako, P.K. Hosamane Guruswamy, Characterization Studies on Graphene-Aluminium Nano composites for Aerospace Launch Vehicle External Fuel Tank Structural Application, Materials 15 (17) (2022) 5907.

[29] M. Hedayatian, K. Vahedi, A. Nezamabadi, A. Momeni, Microstructural and mechanical behavior of Al6061-graphene oxide nano composites, Metals and Materials International 26 (6) (2020) 760–772.

[30] L.I.U. Wenyi, H.U. Xiaohui, L.I. Yapeng, T.A.N.G. Ling, Z.H.A.N.G. Hui, Research progress on preparation technology and strengthening mechanism of graphene reinforced aluminum matrix MMCs, Aviation materials science 43 (1) (2023) 51–59.

[31] Sharma, A., Priyadarshini, A., Sujith, R., Subrahmanyam, M.S., Thomas, P.A., and Gupta, A.K., 2019, November. Effect of Graphene Nanoplatelets Incorporation on Microstructural and Tribological Properties of Aluminium Metal Matrix composites. In ASME International Mechanical Engineering Congress and Exposition (Vol. 59490, p. V012T10A021). American Society of Mechanical Engineers.

[32] B. Sahoo, D. Narsimhachary, J. Paul, Tribological characteristics of aluminium-CNT/graphene/graphite surface nano composites: a comparative study, Surface Topography: Metrology and Properties 7 (3) (2019) 034001.

[33] P. Ashwath, P. Jeyapandiarajan, M. Anthony Xavior, R. verma, N. kumar singh, Varalaxshmi, Heat treating studies of graphene reinforced aluminium metal matrix composite, Materials Today: Proceedings 5 (5) (2018) 11859–11863.

[34] H.P. Kumar, M.A. Xavior, A.P. Joel, J.K. Chakraborty, Effect of flake reinforcement on mechanical properties of AA 6061 nano composite with secondary nano platelet-Graphene processed through powder metallurgy, Materials Today: Proceedings 5 (2) (2018) 6626–6634.

[35] Y. Xie, X. Meng, Y. Huang, J. Li, J. Cao, Deformation-driven metallurgy of graphene nanoplatelets reinforced aluminum MMC for the balance between strength and ductility, composites Part B: Engineering 177 (2019) 107413.

[36] Z. Zheng, X.X. Yang, J.C. Li, X.X. Zhang, I. Muhammad, G.E.N.G. Lin, Preparation and properties of graphene nanoplatelets reinforced aluminum MMCs, Transactions of Nonferrous Metals Society of China 31 (4) (2021) 878–886.

[37] M. Tabandeh-Khorshid, A. Kumar, E. Omrani, C. Kim, P. Rohatgi, Synthesis, characterization, and properties of graphene reinforced metal-matrix nano composites, Composites Part B: Engineering 183 (2020) 107664.